Absorbing state transition in a one-dimensional contact replication process

S. C. Ferreira, Jr.*
Departamento de Física, Universidade Federal de Viçosa, 36571-000, Viçosa, Minas Gerais, Brazil
(Received 19 May 2004; published 29 September 2004)

In this work, the contact process (CP) is modified in order to model a contact replication process (CRP) for monoclonal reproduction. The occupation rates of an empty site depend on the nearest-neighbor and next-nearest-neighbor sites. The CRP exhibits an absorbing state transition studied through cluster approximations and Monte Carlo simulations. The critical rate obtained from simulations, $\lambda_c = 2.0263(4)$, is smaller than that for CP. However, the CRP critical exponents are in agreement with those for CP and, consequently, the model belongs to the directed percolation universality class.

DOI: 10.1103/PhysRevE.70.036119 PACS number(s): 05.70.Ln, 05.65.+b, 02.50.Ey

I. INTRODUCTION

The simplest example of a nonequilibrium model with an absorbing state transition is the contact process (CP), a model initially proposed as an idealized epidemic [1]. In this model, individuals lying on a lattice can die at rate 1 whereas empty sites are occupied at rate $k\lambda/q$. Here, k is its number of occupied nearest-neighbor (NN) sites and q is the coordination number of the lattice. As the ratio of infection and death increases, the system exhibits a critical phase transition from an empty to an active state. It is a well-known fact that the CP belongs to the directed percolation (DP) universality class [2,3]. For a review about contact process and DP universality class see Refs. [4–6].

Due to its importance as a fundamental model, several CP generalizations were proposed [7,8,10–14]. One of them is the one-dimensional θ-contact process [7], in which the rate for filling an empty site with two occupied NN sites is $\theta\lambda$ while the occupation rate of an empty site with one occupied NN site is $\lambda/2$ (CP is the particular case $\theta=1$). Other examples are the diffusive CP [8], in which particles execute NN hoppings at a rate D, the conservative CP, in which the number of particles does not vary [9], and processes with multiparticle creation [10] and annihilation [11]. All these models preserve the DP universality class. Another group whose static behavior falls in the DP class includes models with an infinity number of absorbing configurations [12–14]. But for these models the time-dependent behavior, associated with the spread of activity from a localized seed, varies continuously with the initial particle density [13,15,16].

A common feature for all mentioned models is that the flow of the infection is equally divided among all the neighbors of the contaminated individuals. This is a reasonable hypothesis for a model of epidemics, but not adequate for a model of monoclonal replication such as in tumor or bacterial growth [17]. Actually, in these cases it is more realistic to suppose a flow of the new cells divided just among the empty neighbors [18]. The simplest model for monoclonal replication is the Williams and Bjerknes (WB) model [19] that considers death and reproduction only for cells with at least one empty neighbor. The WB model does not belong to the DP universality class. In the present work, we consider a one-dimensional contact replication process (CRP), a mix of the WB model and the contact process, in which only cells with at least one empty neighbor replicate at rate λ but any one cell dies at rate 1. As discussed in the next section, this CRP introduces a next-nearest-neighbor (NNN) dependence for the occupation rate of an empty site.

This paper is organized as follows. In Sec. II the details of the CRP model are presented. In Sec. III we discuss a mean field analysis of CRP through cluster approximations. In Sec. IV, Monte Carlo simulations are considered. Finally, some conclusions are drawn in Sec. V.

II. MODEL

As in the original CP, the cells lie on a lattice with periodic boundaries, in which $\sigma_i = \bullet$ represents an occupied and $\sigma_i = \circ$ an empty site. The dynamics of the CRP includes two processes, namely, cell death and reproduction. A cell dies at constant rate 1 (the time is conveniently rescaled). In turn, if a cell has at least one empty NN site, it replicates at rate λ and its daughter cell occupies one of its empty NN sites with equal probabilities. Thus, only cells in "contact" with empty sites can replicate. Notice the subtle but essential difference between CRP and CP. In CP, an occupied site infects each one of its empty NN sites at rate λ/q independently of their number. In contrast, in the CRP the occupation rates depend on the number of empty NN sites. For example, the transition $\bullet\bullet\circ \rightarrow \bullet\bullet\bullet$ has rate $\lambda/2$ in CP and rate λ in CRP. All possible transitions and the respective rates for one-dimensional CRP are shown in Table I. A central feature of the CRP is the NNN dependence for the occupation rate of an empty site, also present in the pair contact process (PCP) [12,14]. However, differently from PCP, CRP has a unique absorbing state. As expected for models with absorbing configurations, if the reproduction rate is not sufficiently larger than the death rate, the absorbing state always is reached and the population vanishes. For the WB model, the critical rate is $\lambda_c^{\mathrm{WB}} = 1$, and a value $\lambda_c^{\mathrm{CP}} \simeq 3.297\,85$ was found for CP. Thus, a critical rate $\lambda_c^{\mathrm{WB}} < \lambda_c < \lambda_c^{\mathrm{CP}}$ defining the absorbing frontier is expected for the present CRP.

The discrete-time formulation of the CRP used in the simulations is the following. At each time step, one occupied

*Electronic address: silviojr@ufv.br

TABLE I. Transitions that contribute to $dp(\bullet)/dt$ or $dp(\bullet\bullet)/dt$.

Transition	Λ	$\Delta N_\bullet$	$\Delta N_{\bullet\bullet}$	N_p
$\circ\hat{\bullet}\circ\rightarrow\circ\hat{\circ}\circ$	1	−1	0	1
$\bullet\hat{\bullet}\circ\rightarrow\bullet\hat{\circ}\circ$	1	−1	−1	2
$\bullet\hat{\bullet}\bullet\rightarrow\bullet\hat{\circ}\bullet$	1	−1	−2	1
$\circ\bullet\hat{\circ}\circ\rightarrow\circ\bullet\hat{\bullet}\circ$	$\lambda/2$	+1	+1	2
$\bullet\bullet\hat{\circ}\circ\rightarrow\bullet\bullet\hat{\bullet}\circ$	λ	+1	+1	2
$\circ\bullet\hat{\circ}\bullet\circ\rightarrow\circ\bullet\hat{\bullet}\bullet\circ$	λ	+1	+2	1
$\bullet\bullet\hat{\circ}\bullet\circ\rightarrow\bullet\bullet\hat{\bullet}\bullet\circ$	$3\lambda/2$	+1	+2	2
$\bullet\bullet\hat{\circ}\bullet\bullet\rightarrow\bullet\bullet\hat{\bullet}\bullet\bullet$	2λ	+1	+2	1

site (a cell) is chosen at random. The chosen cell dies with probability $p=1/(1+\lambda)$. In turn, the cell replicates with probability $1-p$ if at least one of their NN sites is empty. If all the NN sites are occupied, the cell does not replicate. But, if the replication occurs, one of their empty NN sites is occupied with equal probability. After each step, the time is incremented by $\Delta t=1/n$, where n is the number of cells just prior to the event. It is expected that discrete and continuous dynamics differ somewhat at short times, but that both formulations exhibit the same long-time dynamics [4].

III. CLUSTER APPROXIMATIONS

In this section we develop a mean field theory for the CRP using cluster approximations introduced by ben-Avraham and Köhler [20]. These approximations reproduce qualitatively well the phase diagrams, but the critical exponents for low-dimensional systems ($d\leqslant 3$) are incorrect [4]. However, the critical rate for the absorbing state transition approaches the correct value as higher order approximations are considered. The cluster approximation consists of a set of coupled differential equations for the probabilities $p_n(\widetilde{\sigma})$ of a cluster $\widetilde{\sigma}$ with n sites. In general, the transitions of a cluster with n sites depend on the sites outside the cluster. Consequently, the n-site probabilities are coupled with those for m site, where $m>n$, generating an infinity hierarchy [14]. The n-site approximation truncates this hierarchy by approximating m-site probabilities by n-site conditional probabilities. For example, the four-site probability is approximated by

$$p(\sigma_i,\sigma_j,\sigma_k,\sigma_l) \simeq p(\sigma_i|\sigma_j)p(\sigma_j,\sigma_k,\sigma_l) \simeq p(\sigma_i|\sigma_j)p(\sigma_j|\sigma_k)p(\sigma_k,\sigma_l) \quad (1)$$

in the two-site approximation, and

$$p(\sigma_i,\sigma_j,\sigma_k,\sigma_l) \simeq p(\sigma_i|\sigma_j,\sigma_k)p(\sigma_j,\sigma_k,\sigma_l), \quad (2)$$

in the three-site approximation with the conditional probabilities determined by the *Bayes' rule* [21].

A. One-site approximation

The probability rate for an occupied site is given by

$$\frac{d}{dt}p(\hat{\bullet}) = -p(\hat{\bullet}) + \frac{\lambda}{2}p(\hat{\circ}\bullet\circ) + \frac{\lambda}{2}p(\circ\bullet\hat{\circ}) + \lambda p(\hat{\circ}\bullet\bullet) + \lambda p(\bullet\bullet\hat{\circ}), \quad (3)$$

where symbols with the hat designate the site, and symbols without the hat represent its neighborhood. In Eq. (3), the first term represents the particles sinking at rate 1, the second and the third terms represent the occupation rates from the neighbors with an empty neighborhood, and the fourth and fifth terms the occupation from the neighbors with one occupied NN site. By symmetry, $p(\hat{\circ}\bullet\circ)=p(\circ\bullet\hat{\circ})$ and $p(\hat{\circ}\bullet\bullet)=p(\bullet\bullet\hat{\circ})$. Thus, Eq. (3) becomes

$$\frac{d}{dt}p(\bullet) = -p(\bullet) + \lambda p(\circ\bullet\circ) + 2\lambda p(\circ\bullet\bullet). \quad (4)$$

Here, the hats were omitted for the sake of simplicity.

In the one-site approximation, the probability of a microscopic configuration is factorized as $p(\sigma_i,\sigma_j,\sigma_k,\sigma_l,\ldots) \simeq p(\sigma_i)p(\sigma_j)p(\sigma_k)p(\sigma_l),\ldots$, i.e., a simple mean field approximation. Using $p(\bullet)=\rho$ $[p(\circ)=1-\rho]$, where ρ is the mean density of particles, and the one-site approximation in Eq. (4), one finds

$$\frac{d\rho}{dt} = (\lambda-1)\rho - \lambda\rho^3. \quad (5)$$

The last equation has a non-null stationary solution ($d\rho/dt=0$),

$$\rho_s = \sqrt{\frac{\lambda-1}{\lambda}}. \quad (6)$$

Therefore, as in the original CP [4], the critical rate in this approximation is $\lambda_c=1$. In turn, the particle density near the transition scales as $\rho\sim|\Delta|^{-\beta}=|\lambda-\lambda_c|^{-\beta}$, with $\beta=1/2$, a value different from that obtained for the original CP model ($\beta=1$) in the one-site approximation.

Concerning the dynamics of the CRP, the solution of Eq. (5) with the initial condition $\rho(0)=1$ is

$$\rho(t) = \sqrt{\frac{\lambda-1}{\lambda-\exp[-2(\lambda-1)t]}} \quad (\lambda\neq\lambda_c) \quad (7)$$

or

$$\rho(t) = \sqrt{\frac{1}{1+2t}} \quad (\lambda=\lambda_c). \quad (8)$$

Expanding Eq. (7) for long times, we have $\rho-\rho_s \sim \exp(-2\rho_s^2 t)$ for $\lambda>\lambda_c$, leading to a relaxation time

$$\tau = \frac{1}{2\rho_s^2} = \frac{\lambda}{2(\lambda-1)}. \quad (9)$$

Thus, $\tau\sim|\Delta|^{-\nu_\parallel}$, where $\nu_\parallel=1$, the same value of the original CP. At the critical point, the particle density decays asymptotically as $\rho\sim 1/\sqrt{t}$. Therefore, remembering that $\rho(\Delta$

$=0,t)\sim t^{-\delta}$, the critical exponent $\delta=1/2$ is obtained. Notice that the critical exponents in the one-site approximation obey the scaling relation $\delta=\beta/\nu_{\|}$.

B. Two-site approximation

In the two-site approximation the probability of a microscopic configuration is factorized as

$$p(\sigma_i,\sigma_j,\sigma_k,\sigma_l,\ldots)\simeq\frac{p(\sigma_i,\sigma_j)p(\sigma_j,\sigma_k)p(\sigma_k,\sigma_l)\cdots}{p(\sigma_j)p(\sigma_k)\cdots}. \tag{10}$$

The following pair probabilities $\phi=p(\bullet\bullet)$ (both sites are occupied), $\omega=p(\circ\circ)$ (both sites are empty), $\mu=p(\circ\bullet)=p(\bullet\circ)$ (one site is occupied and the other empty) are defined. Moreover, the normalization condition $\phi+\omega+2\mu=1$ and the relation $\rho=\phi+\mu$ reduce the number of independent variables to 2.

Table I contains all processes for which ρ or ϕ change, the correspondent rates (Λ), the variations in the number of particles ($\Delta N_{\bullet}$) and pairs ($\Delta N_{\bullet\bullet}$), and the number of states with the same probability (N_p).

Each transition $\tilde{\sigma}\rightarrow\tilde{\sigma}'$ in Table I contributes to $dp(\bullet\bullet)/dt$ with $p(\tilde{\sigma})\Lambda N_p\Delta N_{\bullet\bullet}$. Using the relation

$$p(\sigma_i,\sigma_j,\sigma_k,\ldots)+p(\sigma_i',\sigma_j,\sigma_k,\ldots)=p(\sigma_j,\sigma_k,\ldots) \tag{11}$$

and the symmetry conditions, the following exact equation is obtained:

$$\frac{d}{dt}p(\bullet\bullet)=-2p(\bullet\bullet)+\lambda[p(\bullet\circ)+p(\bullet\circ\bullet)+p(\bullet\bullet\circ)+p(\bullet\bullet\circ\bullet)]. \tag{12}$$

An analogous procedure for $dp(\bullet)/dt$ leads to Eq. (4).

Using Eq. (10) in Eqs. (4) and (12), we obtain

$$\frac{d\rho}{dt}=-\rho+\lambda\frac{\rho^2-\phi^2}{\rho} \tag{13}$$

and

$$\frac{d\phi}{dt}=-2\phi+\lambda\frac{(\rho^2-\phi^2)(1-\phi)}{\rho(1-\rho)}. \tag{14}$$

The stationary solutions of Eqs. (13) and (14) are

$$\rho_s=2-\sqrt{\frac{\lambda}{\lambda-1}}\ \text{and}\ \phi_s=\sqrt{\frac{\lambda-1}{\lambda}}\rho_s, \tag{15}$$

respectively. Taking $\rho_s=0$ in Eq. (15), the critical rate $\lambda_c=4/3$ is found. Expanding Eq. (15) around λ_c, one finds that $\rho_s\sim(\lambda-\lambda_c)$ and, consequently, $\beta=1$, which differs from the value found in the one-site approximation. A numerical integration of Eqs. (13) and (14) gives $\rho(\Delta=0,t)\sim t^{-1}$ and $\tau\sim|\Delta|^{-1}$ in the asymptotic limit ($t\rightarrow\infty$). Thus, $\delta=1$ and $\nu_{\|}=1$ in agreement with the scaling relation $\delta=\beta/\nu_{\|}$. Notice that the usual mean field exponents for the CP were obtained [4].

C. Three-site approximation

The three-site probabilities are defined as $p(\bullet\bullet\bullet)=a$, $p(\circ\bullet\bullet)=p(\bullet\bullet\circ)=b$, $p(\bullet\circ\bullet)=c$, $p(\circ\bullet\circ)=d$, $p(\bullet\circ\circ)=p(\circ\circ\bullet)=e$, and $p(\circ\circ\circ)=f$. Now, we have 10 unknown variables (including ρ, μ, ω, and ϕ), but the number of independent variables is reduced to four through the following relations:

$$\rho=\phi+\mu,\ \ \phi+2\mu+\omega=1,\ \ a+b=\phi, \tag{16}$$

$$b+d=\mu,\ \ c+e=\mu,\ \ e+f=\omega.$$

Using Eqs. (4) and (12) with the correspondent equations for $dp(\bullet\bullet\bullet)/dt$ and $dp(\circ\circ\circ)/dt$, the stationary density can be evaluated. Thus, from the tables containing all transitions that contribute to da/dt or df/dt the following equations are obtained:

$$\frac{dp(\bullet\bullet\bullet)}{dt}=-3p(\bullet\bullet\bullet)+2\lambda p(\circ\bullet\bullet)+4\lambda p(\bullet\circ\bullet\bullet)+\lambda p(\circ\bullet\circ\bullet\circ) \tag{17}$$

and

$$\frac{dp(\circ\circ\circ)}{dt}=p(\circ\bullet\circ)+2p(\bullet\circ\circ)-\lambda[p(\bullet\circ\circ\circ)+p(\bullet\bullet\circ\circ\circ)]. \tag{18}$$

Substituting the three-site approximation,

$$p(\sigma_i,\sigma_j,\sigma_k,\sigma_l,\sigma_m\ldots)\simeq\frac{p(\sigma_i,\sigma_j,\sigma_k)p(\sigma_j,\sigma_k,\sigma_l)p(\sigma_k,\sigma_l,\sigma_m)\cdots}{p(\sigma_j,\sigma_k)p(\sigma_k,\sigma_l)\cdots}, \tag{19}$$

in Eqs. (4), (12), (17), and (18) we find

$$\frac{d}{dt}\rho=-\rho+\lambda d+2\lambda b, \tag{20}$$

$$\frac{d}{dt}\phi=-2\phi+\lambda(\mu+b+c)+\lambda\frac{bc}{\mu}, \tag{21}$$

$$\frac{da}{dt}=-3a+2\lambda b+4\lambda\frac{bc}{\mu}+\lambda\frac{cd^2}{\mu^2}, \tag{22}$$

and

$$\frac{df}{dt}=d+2e-\lambda\frac{ef}{\omega}-\lambda\frac{bef}{\mu\omega}. \tag{23}$$

The coupled equations were numerically solved providing the critical rate $\lambda_c=1.5550$ and the usual mean field exponents for the CP $\beta=\delta=\nu_{\|}=1$.

The stationary densities ρ_s determined through cluster approximations and Monte Carlo simulations are compared in Fig. 1. The critical rate obtained from Monte Carlo simulations was $\lambda_c\approx2.026$, as described in the next section. So, the critical rate in the n-site approximation approaches the simulated value as larger clusters are considered.

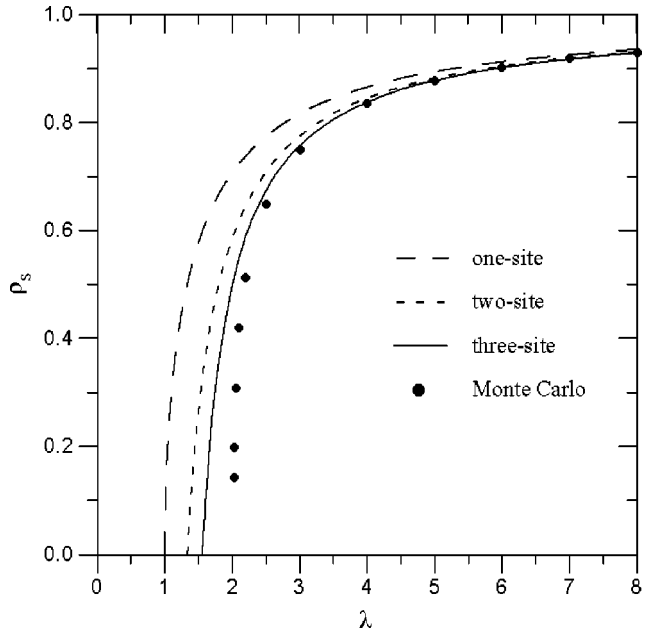

FIG. 1. Stationary densities for cluster approximations and Monte Carlo simulations.

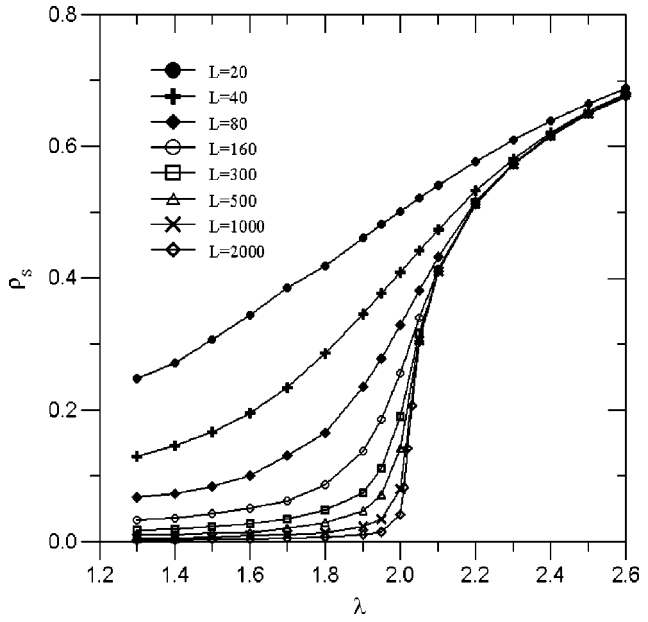

FIG. 2. CRP quasistationary densities versus the replication rate λ. Systems with sizes $L=20-2000$ are shown.

All results for the cluster approximations are summarized in Table II and compared with MC simulations discussed in the next section.

In general, the critical exponents obtained for any mean field approximation have the same values. However, the distinct β and δ values found for the one-site approximation are a peculiarity of the present model. In order to confirm this hypothesis, we generalized the model using a rate $\kappa\lambda$ for the transition $\bullet\bullet\circ \rightarrow \bullet\bullet\bullet$. Notice that for $\kappa=1/2$ ($\kappa=1$) the model reduces to the CP (CRP) process. Now, using the generalized counterpart of Eq. (4), the following equation for the stationary density of particles is obtained:

$$(2\kappa-1)\rho_s^2+2(1-\kappa)\rho_s-\frac{\lambda-1}{\lambda}=0. \tag{24}$$

For any κ value, the critical rate is $\lambda_c=1$. However, for $\kappa \neq 1$,

$$\rho_s=\frac{\Delta}{2|1-\kappa|} \quad \text{for } \Delta=\lambda-\lambda_c\approx 0. \tag{25}$$

Therefore, we have the usual mean field CP exponent $\beta=1$. Moreover, for $\lambda=\lambda_c$ we find $\rho\sim 1/t$ for $t\rightarrow\infty$. Consequently, $\delta=1$. The parameter κ plays a role similar to that of the diffusion rate D in the pair contact process with diffusion (PCPD) [22]. Indeed, PCPD seems to exhibit two distinct universality classes depending on the D value in the two-site approximation.

TABLE II. Summary of the critical parameters for CRP obtained through cluster approximations and Monte Carlo simulations. The numbers in parentheses represent the uncertainties.

	One site	Two site	Three site	MC
λ_c	1	4/3	1.5550	2.0263(4)
β	1/2	1	1	0.273(4)
$\nu_\parallel$	1	1	1	1.71(7)
δ	1/2	1	1	0.159(1)

IV. MONTE CARLO SIMULATIONS

The model was simulated in one-dimensional lattices with sizes ranging from $L=20$ to $L=10\,000$. At the beginning of the simulations, all sites are occupied and a relaxation time t_r preceding the stationary state is used. We estimated the order of t_r as $100L$ and the data were collected in the stationary regime during an interval of length $t_m=2t_r$. The averages were done over N_s independent trials, with N_s ranging from $\sim 10^6$ for the smaller systems to $N_s\sim 10^3$ for the larger ones. Both t_r and t_m were estimated for $\lambda\approx\lambda_c$. Since the only true stationary state of finite systems is the absorbing state, we consider the quasistationary state approach, in which only surviving trials are taken into account [4].

In Fig. 2, the quasistationary density $\overline{\rho_s}$ as a function of λ is shown. This figure suggests a continuous transition from an absorbing state ($\overline{\rho_s}=0$) to an active one when $L\rightarrow\infty$ at $\lambda\approx 2.0$.

To determine the critical rate λ_c, two criteria were employed: the finite-size scaling behavior for the order parameter $\overline{\rho_s}$ and the time-dependent behavior at the critical point [4,5].

For a finite system, $\overline{\rho_s}$ depends on system size and replication rate as [4]

$$\overline{\rho_s}\sim L^{-\beta/\nu_\perp} f(\Delta L^{1/\nu_\perp}), \tag{26}$$

where $f(x)\sim x^\beta$ for large positive x since $\overline{\rho_s}\sim\Delta^\beta$ for $L\gg\xi$, and $\xi\sim|\Delta|^{-\nu_\perp}$ is the correlation length. For large negative x, $f(x)\sim x^{-\nu_\perp+\beta}$ since $\rho(\Delta,L)\sim L^{-1}$. For $\Delta>0$, the density

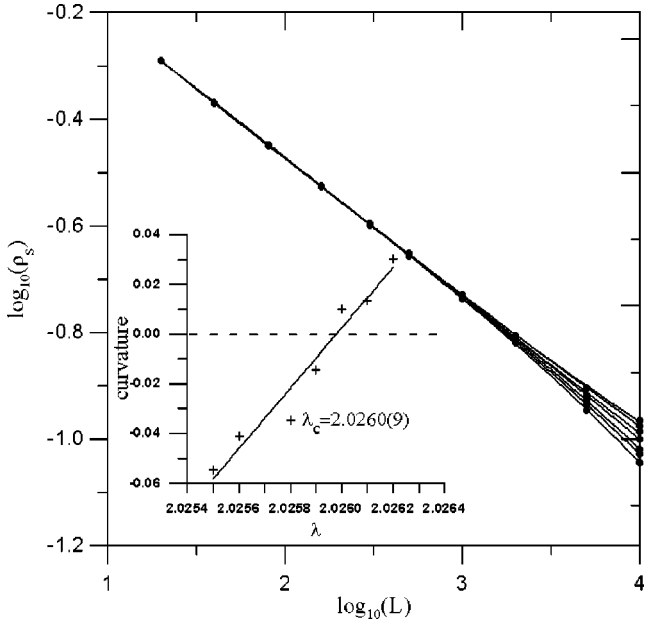

FIG. 3. CRP quasistationary densities versus system size for $\lambda \in [2.0255-2.0262]$ (λ increases from bottom to top). Points represent the simulational data and solid lines the quadratic fits. The inset shows the mean curvature as well as the correspondent linear fit.

reaches a nonzero stationary value, but decreases as L^{-1} for $\Delta<0$. Thus, in the vicinity of the critical point, the double-logarithm plots of $\overline{\rho_s}$ versus L exhibit upward curvatures for $\Delta>0$ and downward curvatures for $\Delta<0$. In order to determine the mean curvature, the double-logarithm data are fitted by a quadratic polynomial P_2 and the mean curvature is defined as

$$\langle \kappa \rangle = \frac{1}{\log L_f - \log L_i} \int_{\log L_i}^{\log L_f} \kappa(x) dx, \tag{27}$$

where $L_i(L_f)$ is the smaller (larger) system size used and $\kappa(x)$ the local curvature defined by the usual formula

$$\kappa = \frac{P_2''}{[1+(P_2')^2]^{3/2}}. \tag{28}$$

We used the data for $L \geqslant 500$ for the quadratic fits. It is important to mention that the quadratic polynomials provide an excellent fitting for all curves with the coefficient of correlation $r^2>0.9999$. The double-logarithm plots of $\overline{\rho_s}$ versus L and the correspondent curvatures (inset) are shown in Fig. 3. In order to determine the point of zero curvature, the data were extrapolated using a linear fit, and the critical rate obtained was $\lambda_c=2.0260(9)$. Here, and in the rest of the paper, the numbers in parentheses reflect the uncertainties. Notice that the critical rate of one-dimensional CRP is smaller than the CP critical rate $\lambda_c^{\mathrm{CP}}=3.297\,85(2)$ [12]. Indeed, it is expected that $\lambda_c^{\mathrm{CRP}}<\lambda_c^{\mathrm{CP}}$ since the replication rate for some CRP configurations are higher than the replication rates for the same configurations in the CP (e.g., the transition $\bullet\bullet\circ \rightarrow \bullet\bullet\bullet$ occurs at rate λ in the CRP and $\lambda/2$ in the CP).

Nevertheless, intensive simulations at the critical point showed that the critical rate obtained from the last analysis is underestimated. So, the second criterium using the time-dependent behavior became necessary [5]. Now, the simulations start with a single particle at the center of the lattice and *all trials* (surviving or not) are taking into account. The quantities of interest are the survival probability $P_s(t)$, the mean number of cells

$$n(t) = \left\langle \sum_{\vec{r}} \sigma_{\vec{r}}(t) \right\rangle, \tag{29}$$

and the spreading of the population

$$R^2(t) = \frac{1}{n(t)} \left\langle \sum_{\vec{r}} r^2 \sigma_{\vec{r}}(t) \right\rangle \tag{30}$$

at time t [5]. Here, $\langle \cdots \rangle$ represents the averages over all trials and $\vec{r}$ the position of the site measured from the initial seed. Moreover, $\sigma_{\vec{r}}=1$ if the site is occupied and $\sigma_{\vec{r}}=0$, otherwise. At the critical point, it is expected that $P_s \sim t^{\delta}$, $n \sim t^{\eta}$, and $R^2 \sim t^z$ while an upward (downward) curvature is expected for $\Delta>0 (\Delta<0)$. The zero-curvature analysis for $P_s(t)$, $n(t)$, and $R^2(t)$ provides a critical rate $\lambda_c=2.0263(4)$, which is more precise than the previous estimate and, therefore, was adopted as the correct value. Exponents $\delta=0.159(1)$, $\eta=0.312(4)$, and $z=1.26(4)$ were found. These exponents are in good agreement with DP class, namely, $\delta_{\mathrm{CP}}=0.1595$, $\eta_{\mathrm{CP}}=0.3137$, and $z_{\mathrm{CP}}=1.265$ [4].

Returning to the quasistationary analysis in the vicinity of λ_c, we expect that $\rho \sim \Delta^{\beta}$. A finite-size analysis for $L \in [1000, 10\,000]$ gives $\beta=0.274(4)$. This β value is close to the exponent $\beta_{\mathrm{CP}}=0.2765$ for the DP class [4]. Other quantities of interest are the relaxation time τ_ρ and the variance $\chi \equiv L^d(\langle \overline{\rho_s^2} \rangle - \langle \overline{\rho_s} \rangle^2)$ of the quasistationary density. These quantities are defined by

$$\tau_\rho \sim |\Delta|^{-\nu_\parallel} \tag{31}$$

and

$$\chi \sim |\Delta|^{-\gamma}. \tag{32}$$

An evaluation of $\nu_\parallel$ using the definition (31) is not precise due to difficulties in determining τ_ρ for $\lambda \neq \lambda_c$. The exponent obtained using this method was $\nu_\parallel=1.6(3)$. A more reliable determination of the $\nu_\parallel$ will be presented in the next discussion. However, the γ exponent can be readily obtained. A finite-size analysis for $L \in [1000, 10\,000]$, gives $\gamma=0.545(9)$, which agrees with the CP exponent $\gamma_{\mathrm{CP}}=0.5439$ [4].

At the critical point one expects that [4]

$$\tau_\rho \sim L^{\nu_\parallel/\nu_\perp} \tag{33}$$

and

$$\chi \sim L^{\gamma/\nu_\perp}. \tag{34}$$

Here, τ_ρ can be defined as the crossover time in the log $\times$ log plot of $\rho(t)$ versus t (inset of Fig. 4). In Fig. 4, the dependences of $\overline{\rho_s}$, τ_ρ, and χ with the system size at the critical point are shown. As expected, these quantities de-

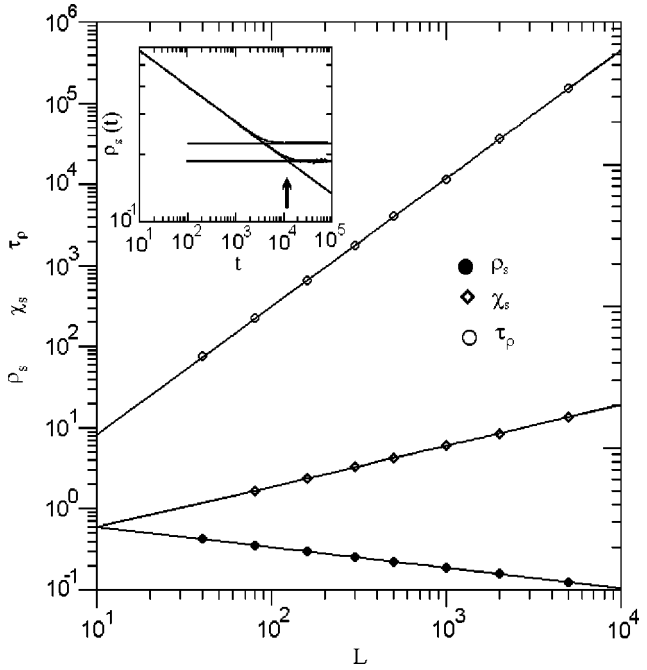

FIG. 4. Mean value, variance, and relaxation time of the quasistationary density at the critical point as a function of the system size. In the inset, examples of the determination of τ_ρ for $L=300$ and $L=1000$ are shown.

pend on the system size as power laws. The correspondent exponents are $\beta/\nu_\perp=0.251(8)$, $\gamma/\nu_\perp=0.503(1)$, and $\nu_\parallel/\nu_\perp=1.581(3)$ which agree with the values $\beta_{\rm CP}/\nu_{\perp_{\rm CP}}=0.2521$, $\gamma_{\rm CP}/\nu_{\perp_{\rm CP}}=0.4958$, and $\nu_{\parallel_{\rm CP}}/\nu_{\perp_{\rm CP}}=1.5808$ obtained for the DP universality class [4]. Using these exponents and the values of β and γ previously determined, we indirectly find a value $\nu_\perp=1.087(4)$. In turn, this value for $\nu_\perp$ leads to $\nu_\parallel=1.72(0)$. Both $\nu_\perp$ and $\nu_\parallel$ are consistent with the CP exponents $\nu_{\perp_{\rm CP}}=1.0968$ and $\nu_{\parallel_{\rm CP}}=1.7338$ [4].

The critical exponents for CRP and CP as well as the perceptual differences among them are shown in Table III. For all exponents, the differences between CRP and CP are of the order of 1% or smaller.

In order to prove the scaling relation (26), we collapsed the data of Fig. 2 plotting $L^{\beta/\nu_\perp}\overline{\rho_s}$ versus $L^{1/\nu_\perp}|\Delta|$. Using the

TABLE III. Critical exponents for CRP [$\lambda_c=2.0263(4)$] and CP [$\lambda_c=3.297\,85(2)$], and the deviation between CRP and CP exponents defined as $|\varepsilon_{\rm CP}-\varepsilon_{\rm CRP}|/\varepsilon_{\rm CP}$, where ε represents the exponent. All CP exponents were taken from Ref. [4] and references therein.

Exponents	CRP	CP	Difference (%)
β	0.274(4)	0.277 649(4)	1.2
γ	0.545(9)	0.543 86(7)	0.4
$\nu_\perp$	1.087(4)	1.096 864(6)	0.8
$\nu_\parallel$	1.72(0)	1.733 83(3)	0.8
δ	0.159(1)	0.159 47(3)	0.2
η	0.312(4)	0.313 68(4)	0.4
z	1.26(4)	1.265 23(3)	0.1

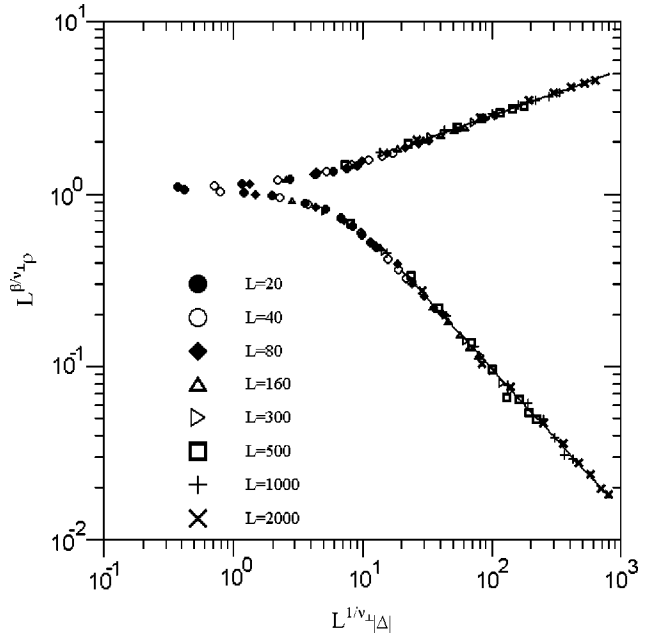

FIG. 5. Collapse of the data presented in Fig. 2.

CRP exponents from Table III and $\lambda_c=2.0263(4)$, an excellent collapse was obtained (Fig. 5). The slope of the upper straight line is 0.269, a value smaller but consistent with the expected value of β. The slope of the lower straight line is −0.818, in excellent agreement with the expected value for DP $-\nu_\perp+\beta\simeq-0.8192$.

In order to complement the simulations, we studied the interface scaling for the CRP at the critical point. This method was introduced by Dickman and Muñoz for the original CP [23]. The height of the interface at a site i is defined as the amount of time that the site i has been occupied. A unitary time step is defined as the implementation of n tentatives in the dynamics of CRP, where n is the number of occupied sites just prior to the step. Thus, the height is defined as $h_i(t)=\Sigma_{t'=0}^{t}s_i(t')$. The width W is defined as $W^2=\langle h^2\rangle-\langle h\rangle^2$. For short times ($t\ll\tau_\rho$) we have $W\sim t^{\beta_W}$ and for long times ($t\gg\tau_\rho$)W reaches a saturation value $W_{\rm sat}\sim L^\alpha$. Moreover, $\tau_\rho\sim L^\zeta$ where $\zeta=\nu_\parallel/\nu_\perp$ [24]. The saturation occurs because all trials are used for sampling and the system certainly reaches an absorbing configuration at the critical point. The last exponents obey the Family-Vicsek scaling relation $\alpha=\beta_W\zeta$ [24]. Also, there is a connection between interface and absorbing transition critical exponents $\beta_W=1-\delta$ and $\alpha=(1-\delta)\nu_\parallel/\nu_\perp$ [23]. Using the CRP exponents we obtain $\beta_W=0.840(9)$ and $\alpha=1.33(0)$. In Fig. 6, a scaling plot of the width averaged over all trials, i.e., W/L^α versus t/L^ζ, using the values $\alpha=1.330$ and $\zeta=1.5813$ expected for the 1D CRP is shown. A very good collapse is observed. The exponent obtained from the linear region of the plot is $\beta_W=0.838(5)$ and the analysis of the saturation width $W_{\rm sat}\sim L^\alpha$ gives $\alpha=1.34(2)$, both in good agreement with the expected values.

V. CONCLUSIONS

In this paper the contact process (CP) was modified in order to model a monoclonal contact replication process

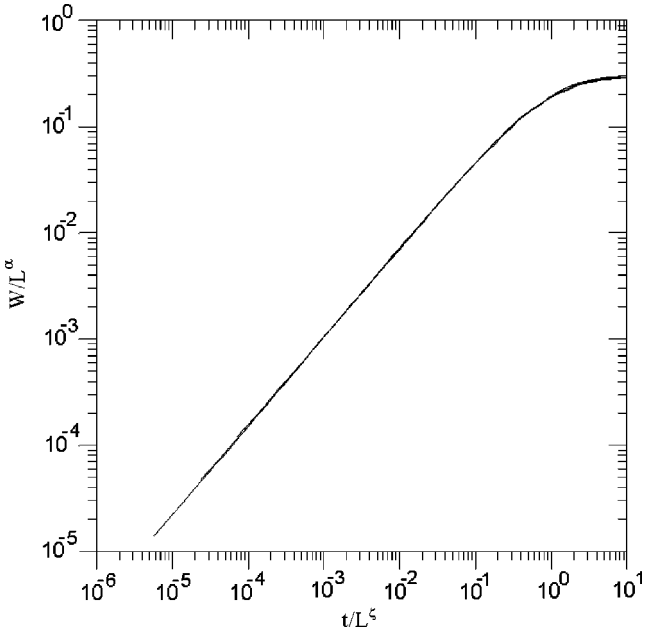

FIG. 6. Collapsed curves for the mean width versus time for CRP with $L=500$, 1000, 2000, 5000.

(CRP). The model was analyzed via cluster approximations and Monte Carlo simulations. One-, two-, and three-site approximations were used and the critical rate approaches the simulated value as larger clusters are considered. The critical exponents in the one-site approximation are $\beta=1/2$, $\delta=1/2$, and $\nu_{\|}=1$, whereas the usual mean-field CP exponents $\beta=\delta=\nu_{\|}=1$ were found for higher cluster approximations.

Monte Carlo simulations provided a critical rate for the absorbing transition $\lambda_c=2.0263(4)$ smaller than that for CP. However, since all exponents are in good agreement with the CP exponents with an error of the order of 1% or smaller, the model is included in the DP class. Our results reinforce the claim that small alterations in the CP rules can strongly affect the critical point but not the critical exponents [4,6]. Indeed, it is a necessary symmetry break, as for example the inclusion of additional absorbing configurations [13], for the occurrence of non-DP behavior. Also, the Williams and Bjerknes (WB) model does not belong to the DP class because it has two absorbing configurations (the vacuum and full configurations). Indeed, at the critical point $\lambda_c^{\mathrm{WB}}=1$ [19] we have that $P_s\sim\sqrt{t}$, $R^2\sim t$, and $n=$const, but a single alteration (death for any cell) leads the model to the DP class. In order to complement this work, the interface scaling properties of CRP were considered. The simulations corroborate the Dickman and Muñoz [23] predictions. The growth and roughness exponents $\beta_W=0.840(9)$ and $\alpha=1.33(0)$ are in good agreement with the CP exponents.

Simulations in two- and three-dimensional lattices will be necessary in order to confirm if the DP class is preserved in higher dimensions. This is not a trivial question because the NNN dependence is more significant at higher dimensions. Also, simple generalizations such as the inclusion of diffusion and source of particles will be considered in the future.

ACKNOWLEDGMENTS

The author thanks José Arnaldo Redinz, Marcelo Lobato Martins, and Mário José de Oliveira for worthy comments. This work was supported by the CNPq-Brazilian agency.

[1] T. E. Harris, Ann. Prob. **2**, 969 (1974).
[2] P. Grassberger and A. de la Torre, Ann. Phys. (N.Y.) **122**, 373 (1979).
[3] R. Dickman and I. Jensen, Phys. Rev. Lett. **67**, 2391 (1993); I. Jensen and R. Dickman, J. Stat. Phys. **71**, 89 (1993).
[4] J. Marro and R. Dickman, *Nonequilibrium Phase Transitions in Lattice Models* (Cambridge University Press, Cambridge, 1999).
[5] R. Dickman, *Nonequilibrium Statistical Mechanics in One Dimension* (Cambridge University Press, Cambridge, 1999).
[6] H. Hinrichsen, Adv. Phys. **49**, 815 (2000).
[7] R. Durret and D. Griffeath, Ann. Prob. **11**, 1 (1983).
[8] M. Katori and N. Konno, Physica A **186**, 578 (1992).
[9] T. Tomé and M. J. Oliveira, Phys. Rev. Lett. **86**, 5643 (2001).
[10] R. Dickman and T. Tomé, Phys. Rev. A **44**, 4833 (1991).
[11] R. Dickman, Phys. Rev. B **40**, 7005 (1989).
[12] I. Jensen, Phys. Rev. Lett. **70**, 1465 (1993).
[13] I. Jensen and R. Dickman, Phys. Rev. E **48**, 1710 (1993).
[14] R. Dickman, W. R. M. Rabêlo, and G. Ódor, Phys. Rev. E **65**, 016118 (2001).
[15] C. López and M. A. Muñoz, Phys. Rev. E **56**, 4864 (1997).
[16] G. Ódor, J. F. F. Mendez, M. A. Santos, and M. C. Marques, Phys. Rev. E **58**, 7020 (1998).
[17] R. A. Weinberg, Sci. Am. **275**, 62 (1996).
[18] A yet more realistic picture must include the division of cells without empty neighbors. But, for this task the effects of stress also must be considered.
[19] T. Williams and R. Bjerknes, Nature (London) **236**, 19 (1972).
[20] D. ben-Avraham and J. Köhler, Phys. Rev. A **45**, 8358 (1992).
[21] N. G. Van Kampen, *Stochastic Processes in Physics and Chemistry* (North-Holland, Amsterdam, 1981).
[22] E. Carlon, M. Henkel, and U. Schollwöck, Phys. Rev. E **63**, 036101 (2001).
[23] R. Dickman and M. A. Muñoz, Phys. Rev. E **62**, 7632 (2000).
[24] A.-L. Barabasi and E. H. Stanley, *Fractal Concepts on Surface Growth* (Cambridge University Press, Cambridge, 1995).